

## In Vivo Distribution of Human Adipose-Derived Mesenchymal Stem Cells in Novel Xenotransplantation Models

TODD E. MEYERROSE,<sup>a</sup> DANIEL A. DE UGARTE,<sup>b</sup> A. ALEX HOFLING,<sup>a</sup> PHILLIP E. HERRBRICH,<sup>a</sup> TAYLOR D. CORDONNIER,<sup>a</sup> LEONARD D. SHULTZ,<sup>c</sup> J. CHRIS EAGON,<sup>d</sup> LOUISA WIRTHLIN,<sup>a</sup> MARK S. SANDS,<sup>a</sup> MARC A. HEDRICK,<sup>b,e</sup> JAN A. NOLTA<sup>a</sup>

<sup>a</sup>Washington University School of Medicine, Division of Oncology, Hematopoietic Development and Malignancy Section, St. Louis, Missouri, USA; <sup>b</sup>UCLA School of Medicine, Department of Surgery, Regenerative Bioengineering and Repair Laboratory, Los Angeles, California, USA; <sup>c</sup>The Jackson Laboratory, Bar Harbor, Maine, USA; <sup>d</sup>Washington University School of Medicine, Division of General Surgery, Department of Surgery, St. Louis, Missouri, USA; <sup>e</sup>Cytori Therapeutics, Inc., San Diego, California, USA

**Key Words.** Adult stem cells • Xenogeneic stem cell transplantation • Stem cell transplantation • Mesenchymal stem cells  
In vivo tracking • Immunodeficient mouse • Human • Ex vivo gene transfer

### ABSTRACT

The potential for human adipose-derived mesenchymal stem cells (AMSC) to traffic into various tissue compartments was examined using three murine xenotransplantation models: nonobese diabetic/severe combined immunodeficient (NOD/SCID), nude/NOD/SCID, and NOD/SCID/MPSVII mice. Enhanced green fluorescent protein was introduced into purified AMSC via retroviral vectors to assist in identification of cells after transplantation. Transduced cells were administered to sublethally irradiated immune-deficient mice through i.v., intraperitoneal, or subcutaneous injection. Up to 75 days after transplantation, tissues were harvested and DNA polymerase chain reaction (PCR) was performed for specific vector sequences as well as for human Alu repeat sequences. Duplex quantitative PCR using human  $\beta$ -globin and murine rapsyn primers assessed the contribution of human cells to each tissue. The use of the novel

NOD/SCID/MPSVII mouse as a recipient allowed rapid identification of human cells in the murine tissues, using an enzyme reaction that was independent of surface protein expression or transduction with an exogenous transgene. For up to 75 days after transplantation, donor-derived cells were observed in multiple tissues, consistently across the various administration routes and independent of transduction parameters. Tissue localization studies showed that the primary MSC did not proliferate extensively at the sites of lodgement. We conclude that human AMSC represent a population of stem cells with a ubiquitous pattern of tissue distribution after administration. AMSC are easily obtained and highly amenable to current transduction protocols for retroviral transduction, making them an excellent avenue for cell-based therapies that involve a wide range of end tissue targets. *STEM CELLS* 2007;25:220–227

### INTRODUCTION

MSC were initially described as a population of colony-forming cells isolated from the bone marrow, capable of differentiation along osteogenic, chondrogenic, adipogenic, and myogenic lineages [1–7]. In the bone marrow, MSC create a “niche” micro-environment for the support of hematopoietic stem cells (HSCs) [8, 9] through integrin engagement, formation of extracellular matrix (ECM), and cytokine secretion (reviewed in [10]). This ability to support hematopoiesis has been exploited in models of bone marrow transplantation using i.v. coadministration of either unmanipulated [11–14] or gene-modified [15–17] MSC. Investigations into the post-transplant fate of marrow-derived MSC have shown evidence of homing to multiple organs in rodents, fetal sheep, nonhuman primates, and humans [18–20]; however, there is limited evidence for efficient rehoming to the marrow niche [21].

In recent years, several investigators have identified similar populations of pluripotent mesenchymal cells resident in various

tissue compartments, including dental pulp [22], skeletal muscle [23], bone [24, 25], and adipose tissue [26–28]. Adipose tissue compartments remain an especially attractive source of MSC due to their ease of harvest, clonogenic potential [29], and robust proliferative capacity [30]. Although adipose-derived MSC (AMSC) retain the same degree of cell surface heterogeneity as cells isolated from the marrow, several investigators have identified consistent differences in cell surface molecule presentation which may influence in vivo trafficking [31–34]. For this study, we have isolated a cell population from human subcutaneous fat that is highly enriched for AMSC consistently expressing the phenotype CD45<sup>-</sup>, CD105<sup>+</sup>, CD44<sup>+</sup>, and CD271<sup>+</sup>.

Here, we have used three strains of immune-deficient mice to examine the post-transplant fate of AMSC after i.v., subcutaneous, or intraperitoneal administration. Human AMSC were expanded ex vivo, retrovirally labeled to express enhanced green fluorescent protein (eGFP), and purified by fluorescence-activated cell sorting (FACS) before transplantation into suble-

Correspondence: Jan A. Nolta, Ph.D., Washington University School of Medicine, Department of Internal Medicine, Division of Oncology, Hematopoietic Development and Malignancy Section, Southwest Tower, 6th floor, Room 643, 4940 Parkview Place, St. Louis, Missouri 63110, USA. Telephone: 314-362-3123; Fax: 314-362-9333; e-mail: jnolta@im.wustl.edu Received April 20, 2006; accepted for publication August 23, 2006; first published online in *STEM CELLS EXPRESS* September 7, 2006. ©AlphaMed Press 1066-5099/2007/\$20.00/0 doi: 10.1634/stemcells.2006-0243

thally irradiated nonobese diabetic/severe combined immunodeficient (NOD/SCID), NOD/SCID/MPSVII, or nude/NOD/SCID recipients. Animals were sacrificed at various time points up to 75 days after transplant, and both hematopoietic and nonhematopoietic tissues were harvested for evaluation of AMSC bio-distribution and persistence of transgene expression. Results showed that regardless of the route of administration, infused human AMSC were able to migrate to a wide range of tissues and persist for the duration of the study. We found no evidence of significant clonal expansion within any organ examined, although endpoint explant cultures plated from different tissues demonstrated that both colony forming units-fibroblast (CFU-F) capacity and transgene expression were retained.

## MATERIALS AND METHODS

### AMSC

AMSC were obtained from elective liposuction patients as previously described [27] or, alternatively, from abdominal adipose samples removed during elective gastric bypass surgery, under approval of human subjects at the University of Southern California (Los Angeles) and at Washington University (St. Louis). After the surgical procedures, all samples were washed thoroughly with phosphate-buffered saline (PBS) (Invitrogen, Carlsbad, CA, <http://www.invitrogen.com>) followed by ECM digestion in 0.075% collagenase (Worthington Biochemical Corporation, Lakewood, NJ, <http://www.worthington-biochem.com>) for 30 minutes at 37°C. Digestion was neutralized with Dulbecco's modified Eagle's medium (Invitrogen) containing 10% fetal bovine serum (FBS) (HyClone, Logan, UT, <http://www.hyclone.com>). The digested adipose tissue was centrifuged at 1,200g for 10 minutes to obtain a cell pellet. The pellet was then resuspended and filtered through a 70- $\mu$ m nylon screen. Cells were then plated at a density of  $1 \times 10^6$  cells per tissue culture plate (diameter 100 mm) and maintained at subconfluence in Dexter's original medium (DOM) consisting of Iscove's modified Dulbecco's medium with 15% FBS (Atlanta Biomedical, Lawrenceville, GA, <http://www.atlantabio.com>), 15% donor horse serum (HyClone),  $10^{-4}$  M 2-mercaptoethanol (Sigma-Aldrich, St. Louis, <http://www.sigmaaldrich.com>),  $10^{-6}$  M hydrocortisone (Sigma-Aldrich), 50 U/ml penicillin, 50  $\mu$ g/ml streptomycin sulfate, and 2 mM L-glutamine (Invitrogen). Media were removed, and nonadherent cells were flushed away 12–18 hours later followed by refeeding with fresh media. With the exception of lineage differentiation conditions, cells were maintained at subconfluence by dissociation with 0.25% trypsin-EDTA (Sigma-Aldrich) and replating under the same culture conditions at a 1:4 dilution. Lineage differentiation was performed with the Poietics MSC differentiation media (Cambrex Bio Science Walkersville, Inc., Walkersville, MD, <http://www.cambrex.com>) according to the manufacturer's instructions to ensure multilineage differentiation ability.

### Flow Cytometric Analysis/FACS

Cells maintained at subconfluence were harvested using enzyme-free Cell Dissociation buffer (Invitrogen) and resuspended in 2.4G2 hybridoma (HB-197; American Type Culture Collection [ATCC], Manassas, VA, <http://www.atcc.org>) cell-free supernatant to block nonspecific Fc receptor binding. Cells were incubated with monoclonal antibodies against human CD11b, CD18, CD31, CD34, CD38, CD44, CD45, and CD54 (R&D Systems, Inc., Minneapolis, <http://www.rndsystems.com>), CD62L, CD90, CD105, CD106, CD117, CD133, CD144, CD166, CD271, and c-met (R&D Systems, Inc.), and Tie-2 and EPO-R (erythropoietin receptor; R&D Systems, Inc.). All antibodies were obtained from BD Biosciences (San Jose, CA, <http://wwwbdbiosciences.com>) unless otherwise indicated. Cells were incubated with antibody for 30 minutes on ice, washed twice with PBS containing 2% FBS (HyClone), and resuspended in PBS. Flow cytometric analyses were performed using a Cytomics FC500 (Beckman Coulter, Fullerton, CA, <http://www.beckmancoulter.com>), and FACS was performed using a MoFlo

High-speed Cell Sorter (Cytomation, Denver, <http://www.global-spec.com/supplier/profile/cytomation>).

### Retroviral Constructs and Transduction

Retroviral vectors used for the initial transductions were based upon the LXSN backbone originally developed by A. Dusty Miller. More robust production of transgene was elicited from the use of the modified MND LTR developed in Donald Kohn's Vector Core Facility at Childrens Hospital of Los Angeles and characterized in several models [35–37]. The eGFP was inserted into the MND-X-SN backbone to enhance sorting and tracking ability.

Retroviral transduction was performed using vector-containing supernatant from the packaging cell line PA317 as previously described [38]. Briefly, PA317 cells were cultured to 80% confluence under standard conditions at 37°C and then transferred to 32°C for 48 hours. Cell-free supernatant was obtained from these cultures and immediately stored at  $-70^{\circ}\text{C}$  until use. Retroviral titers were approximately  $5 \times 10^6$  infectious virions per milliliter assayed on human cell line HT29 (ATCC).

AMSC received three doses of retroviral supernatant at 24-hour intervals in the presence of 4  $\mu$ g/ml protamine sulfate (Sigma-Aldrich). At least 48 hours after transduction, cell cultures were sorted by FACS for eGFP expression.

### Mice

All animals were housed under sterile conditions in microisolator cages and bred in the Children's Hospital of Los Angeles Department of Lab Animal Resources or in the Washington University Division of Comparative Medicine under approved protocols. NOD-LtSz-scid/scid (NOD/SCID) mice were derived from breeding pairs obtained from The Jackson Laboratory (Bar Harbor, ME, <http://www.jax.org>). NOD-Prkdc<sup>scid</sup>/Prkdc<sup>scid</sup> Foxn<sup>nu</sup>/Foxn<sup>nu</sup> (nude/NOD/SCID) mice were created by extensive crossing of homozygous nude (Foxn<sup>nu</sup>/Foxn<sup>nu</sup>) mice to the NOD/SCID. Generation of the NOD/SCID/MPSVII mouse has been previously described by Hofling et al. [39], and extensive investigation by the group has shown this strain to be equally permissive for human cell engraftment.

Recipient mice received 300 rads of total body irradiation (TBI), followed by administration of MSC within 30 minutes. Mice were sacrificed, and tissues were harvested for analysis up to 75 days after transplantation.

### DNA Extraction and Polymerase Chain Reaction Analysis

Genomic DNA for polymerase chain reaction (PCR) analyses was obtained from tissues by phenol chloroform extraction after a Proteinase K digestion as previously described [40]. The DNA concentration and purity were determined by optical density using a Nanodrop spectrophotometer (NanoDrop Technologies, Wilmington, DE, <http://www.nanodrop.com>) followed by standard DNA PCR or real-time quantitative PCR analysis (TaqMan technology and ABI PRISM 7300; Applied Biosystems, Norwalk, CT, <http://www.appliedbiosystems.com>). Tissues were assessed for the presence of the retroviral-specific eGFP transgene using eGFP forward 5'-TACGGCAAGCTGACCCTGAAGTTC and reverse 5'-CGTCTTGGAAG AAGATGGTGCG primers or the neo cassette forward 5'-ATGCTCTTCGTCCAGATCAT and reverse 5'-AAAGTATCC-ATCATGGCTGAT primers. Both PCR protocols include an initial denaturing step at 95°C for 5 minutes and consist of 30 cycles. The protocol for eGFP is 94°C for 1 minute, 57°C for 2 minutes, and 72°C for 2 minutes, and the protocol for neo PCR is 94°C for 5 minutes, 58°C for 2 minutes, and 72°C for 2 minutes. All samples were run in duplicate with a control sample to amplify the murine  $\beta$ -actin gene.  $\beta$ -Actin controls were run under the same conditions as the primary PCR using the primers 5'-TGACGGGGTACCCCACTGTGCCCATCTA and 3'-CTAGAAGCATTTC GGTG-GACGATGGAGGG.

Quantitative duplex PCR (QPCR) was performed as previously described [11]. Briefly, human  $\beta$ -globin forward primer 5'-GTG-CACCTGACTCCTGAGGAGA-3' and reverse primer 5'-CCTT-GATACCAACCTGCCAG-3' were used in conjunction with the

probe 5'-FAM-AAGGTGAACGTGGATGAAGTTGGTGG-TAMRA-3'. As described, the murine *rapsyn* gene was also amplified to assess the contribution of human cells in each tissue. The primers for the *rapsyn* gene were forward 5'-ACCCACCCATCCT-GCAAAT-3' and reverse primer 5'-ACCTGTCCGTGCT GCA-GAA-3' with an appropriate probe as determined using Primer Express software (Applied Biosystems, Foster City, CA, <https://www2.appliedbiosystems.com>). For all analyses, calibration curves for each product demonstrated greater than 95% amplification efficiency and greater than .97 correlation ( $r^2$ ). QPCR controls included a no-template control, human MSCs only, and extracted organs from irradiated, but not transplanted, animals.

For calculations of organ cellularity and absolute donor cell contributions, DNA was extracted from tissue samples and multiplied by the sample fraction of the total tissue wet weight. Cells were assumed to have an average 6-pg DNA for determination of total organ cellularity. Donor cell frequencies were obtained from the above QPCR protocol.

### Detection of Human Cells: Tissue Analyses

For cytospin slides, tissue samples were mechanically dissociated with tissue homogenizers in a PBS-based solution of 100 mM EDTA and 0.25% Trypsin into single-cell suspensions. These homogenates were filtered through a 70- $\mu$ M sterile mesh filter, diluted to  $1 \times 10^6$  cells per milliliter in 50% FBS, and then centrifuged onto slides using 3 minutes of rotation at 700 rpm. Samples were visualized without fixation under a fluorescence microscope for eGFP-positive cells.

For explant cultures, mouse tissues were mechanically dissociated in the presence of 0.075% collagenase (Worthington Biochemical Corporation), 0.25% trypsin (Sigma-Aldrich), and 1 mM EDTA (Sigma-Aldrich) at 37°C for 1 hour, followed by filtration through a 70- $\mu$ m nylon filter screen and plating onto a T75 flask in complete DOM at a density of approximately  $1 \times 10^6$  cells per  $\text{cm}^2$ . Twelve to 24 hours after plating, nonadherent cells were gently rinsed off, and selection conditions were introduced to the explant cultures using 0.75 mg/ml active G418 (geneticin; Invitrogen) for a selection period of 7–10 days based on 100% killing of nontransduced parallel cohorts. CFU-F from these cultures were enumerated for comparison with data obtained using QPCR.

## RESULTS

### AMSC Culture and Transduction

AMSC cultures obtained from liposuction aspirates, subcutaneous adipose tissue, and gastric bypass surgeries from 11 individual donors were statistically indistinguishable from each other by all assays, and thus, results were combined throughout this study. Lipoaspiration donors in our study yielded approximately 17 g of raw material producing an average of  $1.5 \times 10^7$  total mononuclear cells (MNCs) after density centrifugation. This variability results from unavoidable fluctuations in the aspiration procedure itself, as well as individual patient variability. Similar numbers of both raw material and MNC yield were maintained in samples obtained through resection during elective gastric bypass surgery, again with minor fluctuations due to the procedure itself. From this MNC isolation,  $5 \times 10^4$  cells are plated per  $\text{cm}^2$  in tissue-culture dishes, resulting in 10–20 CFU-F colonies per dish after 5 days. Interestingly, the CFU-F formation rate in our experience does not necessarily correlate with the MNC cellularity of the sample. We attribute this, again, to variability in the aspiration procedure itself and to the introduction of peripheral blood into the adipose sample. Cells from this first adherence were dissociated and replated at a density of approximately  $3.5 \times 10^3$  cells per  $\text{cm}^2$ , with a 75% confluence attained at approximately  $1.6$ – $2.0 \times 10^4$  cells per  $\text{cm}^2$ . At no time during this study were MSC allowed to form sheets of confluent monolayer. As shown in Table 1, initial

**Table 1.** Flow cytometric analysis of fresh and cultured cells

Antibody	Passage 0	Passage 4
CD11b	27.31 $\pm$ 13.77	11.65 $\pm$ 3.2
CD34	50.245 $\pm$ 16.62	2.87 $\pm$ 2.45
CD44	65.0 $\pm$ 15.5	97.3 $\pm$ 2.2
CD45	38.7 $\pm$ 12.4	7.165 $\pm$ 3.41
CD54	12.42 $\pm$ 5.6	31.2 $\pm$ 1.6
CD90	52.8 $\pm$ 8.6	98.2 $\pm$ 1.3
CD105	6.35 $\pm$ 4.8	64.4 $\pm$ 15.1
CD117	1.34 $\pm$ 0.69	0.64 $\pm$ 0.30
CD133	0.38 $\pm$ 0.09	0.115 $\pm$ 0.05
CD271	5.6 $\pm$ 1.8	62.3 $\pm$ 7.5
c-met	1.945 $\pm$ 1.33	11.4 $\pm$ 4.02
ABCG2	26.3 $\pm$ 3.0	2.43 $\pm$ 1.2
EPO-R	8.205 $\pm$ 5.3	5.49 $\pm$ 2.0

Antibodies tested for cell surface phenotyping of AMSC. Passage 0 cells are freshly isolated single cell suspensions prepared from human subcutaneous adipose tissue. Passage 4 shows the enrichment of MSC marker expression after culture. Numbers represent the average percentage of positive cells by flow cytometry  $\pm$  SEM, as determined from gating using the isotype controls.

cultures were highly heterogeneous, containing an average of  $38.7\% \pm 12.4\%$  (mean  $\pm$  SEM) CD45<sup>+</sup> hematopoietic cells. These first passage cultures began log-phase proliferation within 4 days and then maintained a population doubling time of  $76 \pm 7.2$  hours. Transduction conditions (as described in Materials and Methods) were initiated at first passage, with sham-transduced cohorts in parallel. CFU-F frequency and lineage differentiation capacity were compared between donors and between transduced and sham-treated cohorts within each donor set. Limiting dilution cultures revealed donor variability in CFU-F generation; however, both CFU-F frequency and lineage potentiality were in range of previously reported values [27, 29] and showed no effect from the retroviral transduction protocol. After three cycles of virus administration, cultures were returned to complete DOM and allowed to rest at least 48 hours before flow cytometric analysis and purification. Transduction efficiencies ranged from 28% to 46% of the bulk culture, with no statistically significant difference in the CD45<sup>-</sup>, CD105<sup>+</sup>, CD44<sup>+</sup>, CD271<sup>+</sup> subset of cells. At passage 4, cells were highly enriched for MSC, containing  $97.3\% \pm 2.2\%$  CD44<sup>+</sup> cells and showing 10-fold enrichment in both CD105<sup>+</sup> and CD271<sup>+</sup> cells (Table 1). In agreement with previously published results, MSC do not express CD45 [5, 6, 27] and rapidly lose expression of CD34 during culture [41]. AMSC were FACS-sorted for eGFP-expressing cells and contained greater than 97% purity for CD45<sup>-</sup> cells that expressed CD44, CD271, and CD105. FACS-sorted cells were either administered at  $1 \times 10^6$  cells per animal into sublethally irradiated recipients or returned to culture for lineage differentiation assays and transgene expression studies.

### NOD/SCID Strain Variants

The NOD/SCID strain variants were selected as recipients for specific benefits provided by their mutations. Since its original description [42], the NOD/SCID animal has become a widely used model in hematopoietic transplant biology. However, NOD/SCID animals typically succumb to an EMV-30 provirus-related thymic lymphoma that shortens their lifespan to an average of 8.5 months. After the rigors of radiation and transplantation, we found this lifespan to be further decreased to the point that survival past 60 days after transplantation was not reliable. The nude/NOD/SCID strain variant was created in our laboratory through successive crossing of NOD-LtSz-scid/scid to Foxn<sup>nu</sup>/Foxn<sup>nu</sup> animals. This selective breeding was designed to displace the EMV-30 provirus found in the NOD/SCID chromosome 11 with two copies of the nude gene, also located

**Table 2.** Human cell detection by enhanced green fluorescent protein (eGFP) DNA polymerase chain reaction

	NOD/SCID i.v.			NOD/SCI i.p.			NOD/SCID s.c.			NNS i.v.				NNS i.p.				NNS s.c.			
	30 days (n = 3)	45 days (n = 3)	60 days (n = 2)	30 days (n = 3)	45 days (n = 2)	60 days (n = 1)	30 days (n = 3)	45 days (n = 1)	60 days (n = 1)	30 days (n = 4)	45 days (n = 23)	60 days (n = 4)	75 days (n = 3)	30 days (n = 3)	45 days (n = 3)	60 days (n = 3)	75 days (n = 2)	30 days (n = 3)	45 days (n = 3)	60 days (n = 2)	75 days (n = 1)
Intestine	2	2	0	3	1	1	0	0	0	2	2	2	1	3	3	1	0	2	0	1	0
Heart	1	1	0	1	1	1	0	0	0	1	1	1	0	2	1	1	1	1	1	0	1
Spleen	3	2	1	0	0	1	1	0	1	3	0	2	1	2	1	1	1	1	1	1	1
Liver	3	1	1	3	1	1	1	0	1	3	3	3	1	3	1	1	1	1	1	0	1
Lung	3	3	2	3	1	1	2	1	1	4	3	4	3	2	2	2	2	2	2	1	1
Kidney	1	1	1	2	2	1	1	0	1	4	2	3	2	2	3	2	1	2	2	0	0
Muscle	2	1	0	0	0	1	1	1	0	2	0	1	1	2	1	1	0	1	1	1	1
Brain	2	2	1	2	1	1	1	0	1	1	2	2	2	2	2	1	1	2	2	0	1
Fat	2	2	1	3	1	1	2	1	1	1	2	2	2	3	3	3	2	1	0	1	0

The number of animals per cohort that tested positive for eGFP DNA at each time point is shown. All mice received  $1 \times 10^6$  transplanted human adipose MSC via i.v., i.p., or s.c. injection after 300 rads sublethal total body irradiation. The table shows data for NOD/SCID animals up to 60 days post-transplantation and for nude/NOD/SCID mice up to 75 days post-transplantation.

Abbreviations: NOD/SCID, nonobese diabetic/severe combined immunodeficient; NNS, nude/nonobese diabetic/severe combined immunodeficient.

on chromosome 11. The nude/NOD/SCID thus retains a severe immune defect and its concomitant permission of human cell xenotransplant, without the life-shortening propensity for thymoma. As shown in Table 2, the nude/NOD/SCID provided equivalent engraftment potential compared with the NOD/SCIDs with an increased lifespan to allow accumulation of data at later time points.

The NOD/SCID/MPSVII variants have been previously characterized as an equivalent model to the traditional NOD/SCID for hematopoietic transplantation, with the benefit of unequivocal identification of donor cells without reliance upon cell surface protein expression [39, 43]. We and others have observed that MSC can both downregulate and modulate their presentation of many cell-surface molecules, including major histocompatibility complex and human leukocyte antigen-related proteins [21, 44–46]. In one extensive study by Smith et al. from Darwin Prockop's group [47], more than 200 commercial antibodies were screened against developing MSC in vitro without identification of an exclusive, consistent marker of primitive MSC. Because of this ambiguity, we chose to identify donor cells using the biochemical detection of  $\beta$ -glucuronidase, the enzyme that is missing in the NOD/SCID MPSVII strain.

### Detection of Transgene: Cytospin Analysis

Expression of eGFP from the modified MND promoter provides robust (>2 log increase mean fluorescence intensity by FACS) signal with no evidence of methylation-based silencing in several model systems to date [35, 48]. In vitro cohorts were maintained in parallel to transplants to monitor persistence of transgene expression through greater than 20 population doublings. Cytospin analyses were performed from mechanically dissociated tissues harvested at day 75 to confirm retained expression of eGFP post-transplant (Fig. 1) given that the frequency of engrafted human cells was below a limit detectable using flow cytometry. Unfixed cytospin assays were employed to eliminate possible artifact from frozen tissue section autofluorescence, and all cytospins were compared with matched organs from irradiated, nontransplanted animals. Human eGFP-bright cells were observed in the brain, heart, liver, lung, kidney, and omental fat of the majority of animals tested at day 30, regardless of the route of administration (Fig. 1; Table 2).

### Explant Culture

At all time points, mechanically dissociated organs were filtered and single-cell suspensions were generated for bulk plating.

Adherent monolayers from these ex vivo cultures were selected using G418 as outlined above, and at all time points, eGFP-positive CFU-F were observed at a very low frequency (data not shown). CFU-F were scored as cells able to give rise to discrete colonies of greater than 40 cells. Post-transplantation explant cultures produced minimal CFU-F colonies from all organs, and although the colonies produced met our requirement of greater than 40 cells per CFU-F, none of the explant culture CFU-F colonies was able to robustly proliferate into sufficient cells for extensive multilineage analysis. Although pretransplant lineage potential analysis showed this population of AMSC to generate approximately 1 CFU-F per 5,000 total MNCs, explant cultures revealed a significant decrease in this frequency, generating an average of approximately 1 CFU-F per 15,000 recovered AMSC, based on QPCR data on AMSC per organ divided by the average total cellularity of each organ. This deficiency in colony-forming ability could be the result of the extensive manipulation of cells during explant isolation, apoptotic signaling from the massive cell death during selection, or a number of factors encountered during the transplant or culture period. Of the minimal CFU-F colonies produced, only limited staining for osteogenic or adipogenic potential could be performed using alkaline phosphatase (AP) activity and oil red O, respectively. Minimal cell numbers prevented the generation of high-density cell pellets currently required for cell consolidation and chondrogenesis. These limited studies showed that approximately 50% of the recovered CFU-F were able to display AP activity and that approximately 30% of the clones stained positive by oil red O, consistent with our previously reported potentiality from AMSC [27]. In summary, the ability of the CFU-F recovered from tissues to persist in vitro for several passages after explant suggests that the self-renewal capacity of the AMSC was not exhausted, although conditions for their proliferation both in vivo and in vitro were not optimal.

### DNA PCR for eGFP

Portions of excised organs were collected and snap-frozen on liquid nitrogen. Extracted DNA was assayed using DNA PCR against the eGFP transgene at 30, 45, and 60 days for NOD/SCID and NOD/SCID/MPSVII mice, while the extended lifespan of the nude/NOD/SCID strain allowed these experiments to progress to day 75. Given the extensive characterization of the NOD/SCID/MPSVII strain by Hofling et al. [39, 43] and Young et al. [49] and statistically indistinguishable results in these experiments, NOD/SCID and NOD/SCID/MPSVII ani-

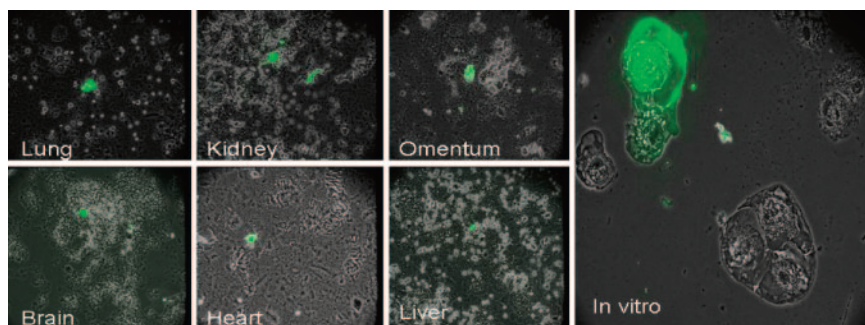


**Figure 1.** Cytospin analysis of adipose-derived mesenchymal stem cells transduced by the MND-eGFP-SN retroviral vector. Cells from a nonselected *in vitro* culture are shown on day 75 after transduction. Tissues were harvested from a nude/nonobese diabetic/severe combined immunodeficient mouse at day 75 and mechanically dissociated for immediate cytospin analysis and fluorescent microscopy. Enhanced green fluorescent protein fluorescence is shown.

mals were combined in these data sets. As shown in a representative eGFP PCR from two nude/NOD/SCID animals (Fig. 2), dissemination of transplanted human AMSC was widespread and showed variable biodistribution, even bilaterally between brain hemispheres of the same animal (Fig. 2, lanes 8 and 9). This variability was seen consistently in all transplant regimens, even when the same donor product was administered to different animals. In this example, the esophagus, adrenal glands, kidney, and bladder displayed a stronger signal in one mouse than the other, although both received identical products and routes of administration (Fig. 2). Similarly, weak signals were detected in the stomach and pancreas of mouse A, but not B, and in the uterus of both animals.

Table 2 shows a compilation of animals assayed for the eGFP transgene from the grouped NOD/SCID and nude/NOD/SCID experiments, illustrating the different routes of administration and time points post-transplantation. Although the human cells had trafficked to various organs, we were unable to detect AMSC in the peripheral circulation at any time point collected. Small numbers of circulating MSC have been detected by other investigators at early time points, using a nonhuman primate model with large numbers of infused cells [50]; however, the mechanisms surrounding this observation have not been described. In accord with other studies involving human xenotransplantation in rodents, we did not observe rehoming of the transplanted cells to the marrow niche at any time point.

### In Situ Tissue Analysis

As noted previously, autofluorescence of frozen tissue sections obscured identification of eGFP fluorescence. To detect resident human cells within the tissue architecture, we examined frozen sections of NOD/SCID/MPSVII organs using a biochemical assay exploiting the activity of  $\beta$ -glucuronidase, the enzyme that is absent in this mouse model. The use of a naphthol-AS-BI- $\beta$ -D-glucuronide substrate as previously described [39] results in deposition of a bright red color over any enzymatically normal cell. Methyl-green counterstaining of nuclei allowed enumeration of donor cells per field using light microscopy (Fig. 3). Figure 3A shows a  $\times 10$  field from a transplanted NOD/SCID/MPSVII kidney section, demonstrating the sparse distribution of human AMSC. The same low-level seeding was observed in all tissues observed, with the highest cell counts observed in lung at the 30-day time points (Fig. 3B). This method of cell detection was used to screen for clonal expansion of AMSC at the site of lodgement and was preferable to traditional immunostaining techniques due to its resistance to background and nonspecific staining in difficult organs such as spleen and liver (Fig. 3C, 3D). These images are representative of  $\times 10$  fields containing positive events and do not indicate this frequency of events in every section of each tissue. The frequencies of both total donor cells per organ and CFU-F-competent cells per organ

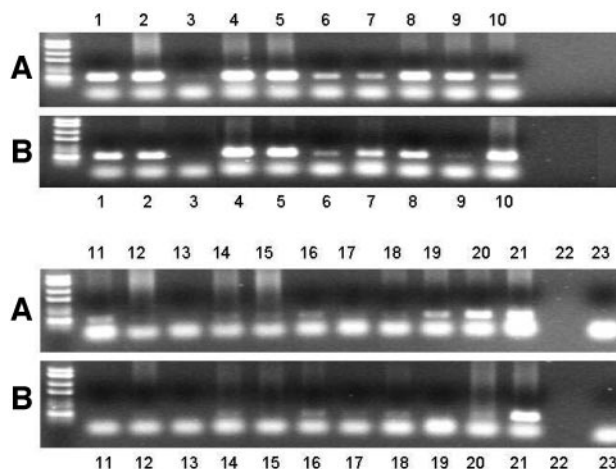


**Figure 2.** Semiquantitative polymerase chain reaction for the enhanced green fluorescent protein gene in human adipose-derived mesenchymal stem cells that had trafficked to various tissues in nude/nonobese diabetic/severe combined immunodeficient mice A and B after intraperitoneal injection. Tissues were harvested after perfusion at day 30 postinjection. The following tissues are shown: (1) heart, (2) lung, (3) trachea, (4) pectoralis muscle, (5) femoral muscle, (6) inguinal fat, (7) uterus, (8) left brain hemisphere, (9) right brain hemisphere, (10) positive control, (11) esophagus, (12) duodenum, (13) colon, (14) stomach, (15) pancreas, (16) liver, (17) spleen, (18) adrenal gland, (19) kidney, (20) bladder, (21) omental fat, (22) blank, and (23) reagents alone.

were determined precisely using QPCR and explant culture under drug selection; however, the observed positive events by biochemical detection were correlative with the number obtained through these other methods.

### Quantitation of Human Cells

A duplex QPCR system was used to quantify the contribution of human cells per organ through simultaneous detection of the murine *rapsyn* and human  *$\beta$ -globin* genes [11]. Nontransduced AMSC were transplanted into five sublethally irradiated nude/NOD/SCID animals via intraperitoneal injection with two control transplants that had received AMSC without radiation conditioning. Animals were sacrificed at 75 days, followed by harvest of peripheral blood, bone marrow, spleen, pancreas, kidney, liver, lung, muscle, brain, and heart. Organs were mechanically dissociated and homogenized, and DNA was extracted, and 100 ng per organ was used for QPCR. Absolute standard curves were generated for evaluation of QPCR results using replicates of 10-fold dilutions of both human and murine DNA within purified extracted DNA from the opposite species. In this fashion, we were able to detect as little as 0.005 ng of either species' DNA within 100 ng of total DNA from the alternate species. Given an average of 5 pg of DNA per cell, this represents the detection of one cell per 100,000, or approximately

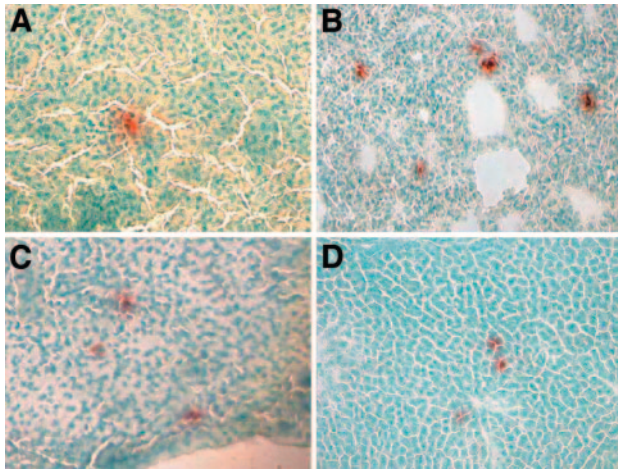


**Figure 3.** Tissue sections from sublethally irradiated nonobese diabetic/severe combined immunodeficient/MPSVII immunodeficient mice transplanted intravenously with human adipose-derived mesenchymal stem cells. Mice were anesthetized and perfused prior to tissue harvest, and cryosections were made. Sections were stained for the  $\beta$ -glucuronidase enzyme activity using naphthol-AS-BI- $\beta$ -D-glucuronide as the substrate (red) and then were counterstained with methyl green. Examples of tissue slides stained using this method are shown. (A): Kidney. (B): Lung. (C): Spleen. (D): Liver.

0.001% engraftment. Results are expressed as the mean number of human cells per 10,000 murine cells, under the assumption that normal diploid human and murine cells contain equivalent DNA per cell (Fig. 4). Absolute human donor cell contribution per organ was calculated as described in the Materials and Methods to estimate total persisting AMSC and to further rule out the possibility of extensive peripheral proliferation (Table 3).

It was possible to detect transplanted MSC in animals that had not received irradiation; however, the levels were below the limit of quantitation using our QPCR strategy in most tissues. Significant seeding was seen in the lung after transplant and was presumed to be a filtration phenomenon as opposed to a specific migration to this area, a hypothesis supported by histological examination of lung sections from control transplants (data not shown). The results show a wide range of human cell dispersal in all tissues tested, with the notable exceptions of peripheral blood and bone marrow. As suggested by the eGFP PCR data, the highest levels of human cell contribution were found in the lung ( $36.95 \pm 5.039$ ) and spleen ( $15.07 \pm 0.5934$ ), with minimal contribution to the heart and skeletal muscle ( $1.552 \pm 0.09385$  and  $0.07588 \pm 0.5597$ , respectively). Consistent with the results in Table 2, the contribution to the same tissues by the same input donor cells varied widely between transplant recipients (Fig. 4). Taken together, these two data sets indicate that the transduction protocol did not affect the differential tissue repopulation in this transplant model.

## DISCUSSION

The results of our investigations indicate that we have isolated a population of AMSC that are very similar to traditional bone marrow-derived MSC in phenotype, potentiality, and migration kinetics in vivo. Although several investigators have reported the ability of MSC to engraft in certain experimental models including rodents [11, 51], fetal sheep [52], and baboons [19, 50], this is the first study to our knowledge to quantify the contribution of human AMSC to various tissues after transplantation in an immune-deficient mouse model. Mechanisms directing the in vivo homing and

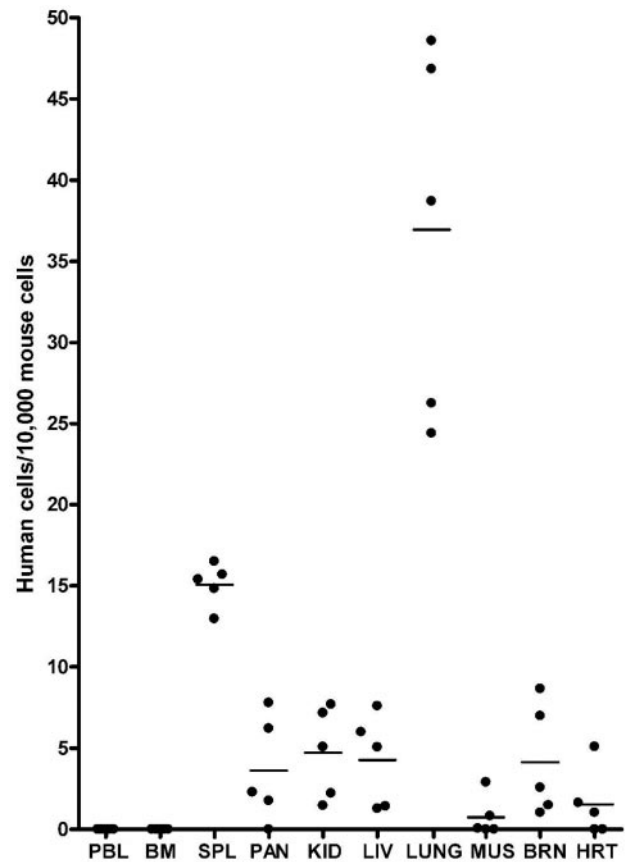


**Figure 4.** Duplex quantitative polymerase chain reaction (PCR) detecting human cells per 10,000 mouse cells. Results from five nude/nonobese diabetic/severe combined immunodeficient animals sacrificed 75 days after sublethal irradiation and intraperitoneal administration of  $1 \times 10^6$  adipose-derived mesenchymal stem cells are shown. Quantitative duplex PCR detects the human  $\beta$ -globin gene and murine *rapsyn* gene simultaneously. All runs were completed with efficiency of more than 95% and  $r^2$  of more than .966. Results are expressed as human cells per 10,000 mouse cells, with mean values  $\pm$  SEM. Abbreviations: BM, bone marrow; BRN, brain; HRT, heart; KID, kidney; LIV, liver; LUNG, lung; MUS, muscle; PAN, pancreas; PBL, peripheral blood.

engraftment of adipose-derived stem cells are not well described and certainly depend on complex interactions between many signaling events. Our data suggest that there is no significant difference in the tissue distribution observed after human AMSC are introduced via any of the three routes of administration tested. This particular result provides an interesting comparison with previous work done in rodent systems examining the distribution and homing of MSCs to various tissue beds. Reports from Gao et al. [53] and Rombouts et al. [54] have demonstrated the efficient trafficking of rodent MSCs to various target organs after transplantation, with a major portion of the input cells retained in the lung. Although this data correlates nicely with our findings, the rodent transplant regimens employed in these studies allowed not only trafficking to multiple tissue beds, but also the return of MSCs to long bones, a result we could not observe in the human xenotransplantation system. The paper by Rombouts et al. [54] also discovered a defect in marrow rehomeing after MSC expansion in culture. Although our preliminary studies with freshly isolated human AMSCs were unable to observe marrow rehomeing in the rodent (data not shown), the widespread distribution of human cells further suggests that even culture-expanded human AMSCs have the ability to navigate in vivo either intravenously or extravascularly and

**Table 3.** Calculation of absolute numbers of donor cells

Organ	Total tissue weight (g)	SEM	Total organ DNA content (ng)	Avg organ cellularity	Frequency of donor cells	Calculated total donor cells per organ	SEM
Spleen	$4.64 \times 10^{-2}$	0.012129487	$4.33 \times 10^5$	$7.21 \times 10^7$	15.07	$1.09 \times 10^5$	$1.20 \times 10^4$
Pancreas	$1.61 \times 10^{-1}$	0.026059995	$2.11 \times 10^6$	$3.51 \times 10^8$	3.618	$1.27 \times 10^5$	$2.37 \times 10^4$
Kidneys	$3.32 \times 10^{-1}$	0.043239848	$2.08 \times 10^6$	$3.46 \times 10^8$	4.73	$1.64 \times 10^5$	$3.93 \times 10^4$
Liver	$1.16 \times 10^0$	0.045045804	$4.55 \times 10^6$	$7.58 \times 10^8$	4.274	$3.24 \times 10^5$	$5.92 \times 10^4$
Heart	$1.35 \times 10^{-1}$	0.007697258	$3.39 \times 10^5$	$5.65 \times 10^7$	1.552	$8.76 \times 10^3$	$1.43 \times 10^3$
Lungs	$1.57 \times 10^{-1}$	0.014706159	$1.27 \times 10^6$	$2.11 \times 10^8$	36.95	$7.80 \times 10^5$	$4.93 \times 10^5$
Brain	$4.62 \times 10^{-1}$	0.028019656	$8.96 \times 10^5$	$1.49 \times 10^8$	4.15	$6.19 \times 10^4$	$1.43 \times 10^4$
Skeletal tissue	$9.32 \times 10^0$	0.224470342	$1.02 \times 10^7$	$1.70 \times 10^9$	0.7588	$1.29 \times 10^5$	$2.63 \times 10^4$

Calculations were made by extracting DNA from tissue samples and multiplying total DNA content by the sample fraction of the total tissue wet weight. Cells were assumed to have an average of 6 pg of DNA, and values are expressed with SEM for sample  $n = 3$ . The frequency of donor cell content was determined in Figure 4 by quantitative polymerase chain reaction as described.

that there are not significant microenvironmental differences in the strains of mice tested to affect this trafficking.

When compared with existing data in the field, our results suggest that the cell surface phenotype differences between adipose-derived and marrow-derived MSCs do not affect the tissue biodistribution to a significant degree, at least at the time points collected. It is possible that the differences in cell surface protein expression have consequences on the early kinetics of MSC dispersal; however, a more basic question still unanswered is whether the trafficking to various tissues is governed by cell autonomous or stochastic processes. In our model, the tracking of AMSCs may be influenced by the administration of TBI. The inability of NOD/SCID strains to deal efficiently with the DNA damage from radiation may cause global inflammatory and cytokine responses that are influencing human cell migration.

Although the AMSC repopulation observed in our studies is not robust in the same manner as a hematopoietic graft, our results have implications for the utility of AMSCs in gene therapy or cell-based therapy applications. Gene-modified AMSCs in this study maintained transgene expression for 75 days and retained their lineage differentiation ability through the transduction protocol. The primary purpose of the marker gene was to demonstrate the ability of MSCs to maintain transgene expression after transplantation and seeding into multiple diverse tissue types. A major limitation in HSC therapy has been the inefficiency of gene transfer protocols into the quiescent stem cell pool to achieve a durable engraftment of corrected cells. This study demonstrates the potential cell therapy utility of easily obtained human MSCs to accept a retroviral transduction, maintain transgene expression, and remain viable in multiple tissue types for an extended period of time. Furthermore, the level of engraftment observed may be sufficient in certain models of disease or injury. Studies on osteogenesis imperfecta by Horwitz et al. [55] have demonstrated cross-correction of disease with detection of less than 2% donor-derived cells.

Bartholomew et al. [56] have described the utility of MSCs in immunomodulation and skin graft survival using a nonhuman primate model with low levels of reported engraftment. Finally, Koc et al. [57] have demonstrated clinical benefit in treatment of lysosomal and peroxisomal deficiencies after infusion of MSCs, without replacement of the marrow niche by donor cells. Our laboratory, and others, have shown marrow-derived MSCs to be highly useful in cotransplantation studies with small numbers of highly purified HSCs, particularly when genetically engineered to secrete supraphysiological levels of protein [16, 17, 58].

Our studies demonstrate that AMSCs possess many of the same phenotypic and functional attributes of bone marrow-derived MSCs. Transplantation into three different strain variants of NOD/SCID immune-deficient mice resulted in widespread distribution of donor human cells into multiple organs, regardless of the route of administration or cell culture manipulation for retroviral insertion. The transplanted human AMSCs were able to persist in these tissues for up to 75 days and retained their multilineage potential and clonogenic capacity. AMSCs that received retroviral vectors retained their transgene expression for the duration of this experiment and were qualitatively indistinguishable from nontransduced cells. Finally, previously reported differences in cell surface protein expression compared with marrow-derived MSCs did not significantly influence the in vivo migration after transplant into immune-deficient mice. In total, these data provide evidence supporting the suitability of AMSCs in cellular therapy or gene therapy applications that would benefit from widespread tissue distribution of autologous engineered or normal donor-derived stem cells.

## DISCLOSURES

The authors indicate no potential conflicts of interest.

## REFERENCES

- Friedenstein AJ, Chailakhjan RK, Lalykina KS. The development of fibroblast colonies in monolayer cultures of guinea-pig bone marrow and spleen cells. *Cell Tissue Kinet* 1970;3:393–403.
- Friedenstein AJ, Deriglasova UF, Kulagina NN et al. Precursors for fibroblasts in different populations of hematopoietic cells as detected by the in vitro colony assay method. *Exp Hematol* 1974;2: 83–92.
- Goshima J, Goldberg VM, Caplan AI. The osteogenic potential of culture-expanded rat marrow mesenchymal cells assayed in vivo in calcium phosphate ceramic blocks. *Clin Orthop Relat Res* 1991;262: 298–311.
- Pereira RF, Halford KW, O'Hara MD et al. Cultured adherent cells from marrow can serve as long-lasting precursor cells for bone, cartilage, and lung in irradiated mice. *Proc Natl Acad Sci U S A* 1995;92:4857–4861.
- Pittenger MF, Mackay AM, Beck SC et al. Multilineage potential of adult human mesenchymal stem cells. *Science* 1999;284:143–147.
- Majumdar MK, Thiede MA, Mosca JD et al. Phenotypic and functional comparison of cultures of marrow-derived mesenchymal stem cells (MSCs) and stromal cells. *J Cell Physiol* 1998;176:57–66.
- Prockop DJ. Marrow stromal cells as stem cells for nonhematopoietic tissues. *Science* 1997;276:71–74.
- Allen TD, Dexter TM, Simmons PJ. Marrow biology and stem cells. *Immunol Ser* 1990;49:1–38.
- Nilsson SK, Johnston HM, Coverdale JA. Spatial localization of transplanted hemopoietic stem cells: Inferences for the localization of stem cell niches. *Blood* 2001;97:2293–2299.
- Deans RJ, Moseley AB. Mesenchymal stem cells: Biology and potential clinical uses. *Exp Hematol* 2000;28:875–884.
- Bensidhoum M, Chapel A, Francois S et al. Homing of in vitro expanded Stro-1- or Stro-1+ human mesenchymal stem cells into the NOD/SCID mouse and their role in supporting human CD34 cell engraftment. *Blood* 2004;103:3313–3319.

- 12 Noort WA, Kruijselbrink AB, in't Anker PS et al. Mesenchymal stem cells promote engraftment of human umbilical cord blood-derived CD34(+) cells in NOD/SCID mice. *Exp Hematol* 2002;30:870–878.
- 13 Lazarus HM, Haynesworth SE, Gerson SL et al. Ex vivo expansion and subsequent infusion of human bone marrow-derived stromal progenitor cells (mesenchymal progenitor cells): Implications for therapeutic use. *Bone Marrow Transplant* 1995;16:557–564.
- 14 Koc ON, Gerson SL, Cooper BW et al. Rapid hematopoietic recovery after coinfusion of autologous-blood stem cells and culture-expanded marrow mesenchymal stem cells in advanced breast cancer patients receiving high-dose chemotherapy. *J Clin Oncol* 2000;18:307–316.
- 15 Bartholomew A, Patil S, Mackay A et al. Baboon mesenchymal stem cells can be genetically modified to secrete human erythropoietin in vivo. *Hum Gene Ther* 2001;12:1527–1541.
- 16 Dao MA, Pepper KA, Nolte JA. Long-term cytokine production from engineered primary human stromal cells influences human hematopoiesis in an in vivo xenograft model. *STEM CELLS* 1997;15:443–454.
- 17 Nolte JA, Hanley MB, Kohn DB. Sustained human hematopoiesis in immunodeficient mice by cotransplantation of marrow stroma expressing human interleukin-3: Analysis of gene transduction of long-lived progenitors. *Blood* 1994;83:3041–3051.
- 18 Liechty KW, MacKenzie TC, Shaaban AF et al. Human mesenchymal stem cells engraft and demonstrate site-specific differentiation after in utero transplantation in sheep. *Nat Med* 2000;6:1282–1286.
- 19 Devine SM, Cobbs C, Jennings M et al. Mesenchymal stem cells distribute to a wide range of tissues following systemic infusion into nonhuman primates. *Blood* 2003;101:2999–3001.
- 20 Aerts F. Mesenchymal stem cell engineering and transplantation. In: Nolte JA, ed. *Genetic Engineering of Mesenchymal Stem Cells*. Dordrecht, The Netherlands: Kluwer Academic Publishers, 2006:1–44.
- 21 Awaya N, Rupert K, Bryant E et al. Failure of adult marrow-derived stem cells to generate marrow stroma after successful hematopoietic stem cell transplantation. *Exp Hematol* 2002;30:937–942.
- 22 Gronthos S, Mankani M, Brahmi J et al. Postnatal human dental pulp stem cells (DPSCs) in vitro and in vivo. *Proc Natl Acad Sci U S A* 2000;97:13625–13630.
- 23 Qu-Petersen Z, Deasy B, Jankowski R et al. Identification of a novel population of muscle stem cells in mice: Potential for muscle regeneration. *J Cell Biol* 2002;157:851–864.
- 24 Noth U, Osyczka AM, Tuli R et al. Multilineage mesenchymal differentiation potential of human trabecular bone-derived cells. *J Orthop Res* 2002;20:1060–1069.
- 25 Grigoriadis AE, Heersche JN, Aubin JE. Differentiation of muscle, fat, cartilage, and bone from progenitor cells present in a bone-derived clonal cell population: Effect of dexamethasone. *J Cell Biol* 1988;106:2139–2151.
- 26 Wickham MQ, Erickson GR, Gimble JM et al. Multipotent stromal cells derived from the infrapatellar fat pad of the knee. *Clin Orthop Relat Res* 2003;412:196–212.
- 27 Zuk PA, Zhu M, Mizuno H et al. Multilineage cells from human adipose tissue: Implications for cell-based therapies. *Tissue Eng* 2001;7:211–228.
- 28 Tholpady SS, Katz AJ, Ogle RC. Mesenchymal stem cells from rat visceral fat exhibit multipotential differentiation in vitro. *Anat Rec A Discov Mol Cell Evol Biol* 2003;272:398–402.
- 29 Guilak F, Lott KE, Awad HA et al. Clonal analysis of the differentiation potential of human adipose-derived adult stem cells. *J Cell Physiol* 2006;206:229–237.
- 30 De Ugarte DA, Morizono K, Elbarbary A et al. Comparison of multilineage cells from human adipose tissue and bone marrow. *Cells Tissues Organs* 2003;174:101–109.
- 31 Katz AJ, Tholpady A, Tholpady SS et al. Cell surface and transcriptional characterization of human adipose-derived adherent stromal (hADAS) cells. *STEM CELLS* 2005;23:412–423.
- 32 Gronthos S, Franklin DM, Leddy HA et al. Surface protein characterization of human adipose tissue-derived stromal cells. *J Cell Physiol* 2001;189:54–63.
- 33 Mitchell JB, McIntosh K, Zvonice S et al. Immunophenotype of human adipose-derived cells: Temporal changes in stromal-associated and stem cell-associated markers. *STEM CELLS* 2006;24:376–385.
- 34 De Ugarte DA, Alfonso Z, Zuk PA et al. Differential expression of stem cell mobilization-associated molecules on multi-lineage cells from adipose tissue and bone marrow. *Immunol Lett* 2003;89:267–270.
- 35 Halene S, Wang L, Cooper RM et al. Improved expression in hematopoietic and lymphoid cells in mice after transplantation of bone marrow transduced with a modified retroviral vector. *Blood* 1999;94:3349–3357.
- 36 Robbins PB, Yu XJ, Skelton DM et al. Increased probability of expression from modified retroviral vectors in embryonal stem cells and embryonal carcinoma cells. *J Virol* 1997;71:9466–9474.
- 37 Robbins PB, Skelton DC, Yu XJ et al. Consistent, persistent expression from modified retroviral vectors in murine hematopoietic stem cells. *Proc Natl Acad Sci U S A* 1998;95:10182–10187.
- 38 Dao MA, Taylor N, Nolte JA. Reduction in levels of the cyclin-dependent kinase inhibitor p27(kip-1) coupled with transforming growth factor beta neutralization induces cell-cycle entry and increases retroviral transduction of primitive human hematopoietic cells. *Proc Natl Acad Sci U S A* 1998;95:13006–13011.
- 39 Hofling AA, Vogler C, Creer MH et al. Engraftment of human CD34+ cells leads to widespread distribution of donor-derived cells and correction of tissue pathology in a novel murine xenotransplantation model of lysosomal storage disease. *Blood* 2003;101:2054–2063.
- 40 Laird PW, Zijderveld A, Linders K et al. Simplified mammalian DNA isolation procedure. *Nucleic Acids Res* 1991;19:4293.
- 41 Simmons PJ, Torok-Storb B. CD34 expression by stromal precursors in normal human adult bone marrow. *Blood* 1991;78:2848–2853.
- 42 Shultz LD, Schweitzer PA, Christianson SW et al. Multiple defects in innate and adaptive immunologic function in NOD/LtSz-scid mice. *J Immunol* 1995;154:180–191.
- 43 Hofling AA, Devine S, Vogler C et al. Human CD34+ hematopoietic progenitor cell-directed lentiviral-mediated gene therapy in a xenotransplantation model of lysosomal storage disease. *Mol Ther* 2004;9:856–865.
- 44 Peister A, Mellad JA, Larson BL et al. Adult stem cells from bone marrow (MSCs) isolated from different strains of inbred mice vary in surface epitopes, rates of proliferation, and differentiation potential. *Blood* 2004;103:1662–1668.
- 45 Stewart K, Walsh S, Screen J et al. Further characterization of cells expressing STRO-1 in cultures of adult human bone marrow stromal cells. *J Bone Miner Res* 1999;14:1345–1356.
- 46 Gronthos S, Zannettino AC, Graves SE et al. Differential cell surface expression of the STRO-1 and alkaline phosphatase antigens on discrete developmental stages in primary cultures of human bone cells. *J Bone Miner Res* 1999;14:47–56.
- 47 Smith JR, Pochampally R, Perry A et al. Isolation of a highly clonogenic and multipotential subfraction of adult stem cells from bone marrow stroma. *STEM CELLS* 2004;22:823–831.
- 48 Wang L, Robbins PB, Carbonaro DA et al. High-resolution analysis of cytosine methylation in the 5' long terminal repeat of retroviral vectors. *Hum Gene Ther* 1998;9:2321–2330.
- 49 Young PP, Vogler C, Hofling AA et al. Biodistribution and efficacy of donor T lymphocytes in a murine model of lysosomal storage disease. *Mol Ther* 2003;7:52–61.
- 50 Devine SM, Bartholomew AM, Mahmud N et al. Mesenchymal stem cells are capable of homing to the bone marrow of non-human primates following systemic infusion. *Exp Hematol* 2001;29:244–255.
- 51 Nilsson SK, Dooner MS, Weier HU et al. Cells capable of bone production engraft from whole bone marrow transplants in nonablated mice. *J Exp Med* 1999;189:729–734.
- 52 Almeida-Porada G, Porada CD, Tran N et al. Cotransplantation of human stromal cell progenitors into preimmune fetal sheep results in early appearance of human donor cells in circulation and boosts cell levels in bone marrow at later time points after transplantation. *Blood* 2000;95:3620–3627.
- 53 Gao J, Dennis JE, Muzic RF et al. The dynamic in vivo distribution of bone marrow-derived mesenchymal stem cells after infusion. *Cells Tissues Organs* 2001;169:12–20.
- 54 Rombouts WJ, Ploemacher RE. Primary murine MSC show highly efficient homing to the bone marrow but lose homing ability following culture. *Leukemia* 2003;17:160–170.
- 55 Horvitz EM, Prockop DJ, Fitzpatrick LA et al. Transplantability and therapeutic effects of bone marrow-derived mesenchymal cells in children with osteogenesis imperfecta. *Nat Med* 1999;5:309–313.
- 56 Bartholomew A, Sturgeon C, Siatskas M et al. Mesenchymal stem cells suppress lymphocyte proliferation in vitro and prolong skin graft survival in vivo. *Exp Hematol* 2002;30:42–48.
- 57 Koc ON, Peters C, Aubourg P et al. Bone marrow-derived mesenchymal stem cells remain host-derived despite successful hematopoietic engraftment after allogeneic transplantation in patients with lysosomal and peroxisomal storage diseases. *Exp Hematol* 1999;27:1675–1681.
- 58 Brouard N, Chapel A, Neildes-Nguyen TM et al. Transplantation of stromal cells transduced with the human IL3 gene to stimulate hematopoiesis in human fetal bone grafts in non-obese, diabetic-severe combined immunodeficiency mice. *Leukemia* 1998;12:1128–1135.